Sizing and control of the energy conversion system of a floating wave energy recovery device based on the oscillating water column principle

João Nicolás Herrero Valério

joao.valerio@tecnico.ulisboa.pt

Instituto Superior Técnico, Universidade de Lisboa, Portugal,
June 2017

Abstract
This paper applies a Discontinuous Galerkin (DG) finite element time-stepping method for the numerical solution of optimal and sub-optimal control problems within the framework of the Pontryagin's Maximum Principle. The local nature of the piecewise polynomial approximation used in the DG method handles easily the case of a large number of switching instants not known *a priori*. The weakly enforced inter-element continuity allows a simple implementation of element-wise mesh and polynomial refinement. To show the capabilities of the method, an element-wise time-interval refinement algorithm was implemented (the so-called h-refinement) and applied to a classic bang-bang optimal control problem. Finally, the application of the method to a practical problem is discussed: the optimal latching (bang-bang) control of a floating oscillating water column wave energy converter equipped with a self-rectifying air-turbine. The results presented in this study show that the DG method is an efficient alternative to the well-known Pseudo-Spectral methods.

Keywords: Discontinuous Galerkin, Pontryagin's Maximum Principle, optimal control, sub-optimal control, bang-bang optimal control

1. INTRODUCTION

The present paper proposes a Discontinuous Galerkin (DG) finite element time-stepping method for the solution of optimal and sub-optimal control problems within the framework of the Pontryagin's Maximum Principle (PMP). The finite element function space normally used by DG approximations consists of piecewise polynomials that are allowed to be discontinuous across element boundaries. The inter-element boundary conditions are weakly enforced. In the present work, the state, co-state and control variables are approximated using Legendre polynomials and the resultant integrals are evaluated using a Gauss-Legendre quadrature rule.

The solution method arising from the DG method only involves a common element-wise matrix due to the weak inter-element boundary conditions.

The numerical solution implies the factorization of a matrix that is equal for all the time-elements, being performed once at the start of the calculations. Mesh refinement, the so-called h-refinement, is straightforward to implement in practice and does not require reassembling the element-wize matrix.

The comparison of Pseudo-Spectral (PS) and DG methods shows that both methods seek a polynomial approximation to the solution and use an integral form of the differential equations. In PS methods, high-order polynomials are usually selected to compute the approximate solution over the whole computational domain. The DG methods satisfy the differential equations in an weak sense, a discretization of the computational domain in multiple finite-elements being preferred in conjunction with the use of lower-order polynomials.

The DG time-stepping method has already been applied to optimal control problems (OCPs) but not in the context of the Pontryagin's Maximum Principle (Boucher et al., 2014a,b; Kraft, 2008; Naveh et al., 1999). In Boucher et al. (2014a,b), the authors only consider one or two time-elements and use high-degree Lagrange polynomials, in a framework similar to the PS methods. Here, a more classic approach is adopted, *i.e.*, lower degree Legendre polynomials and a larger number of finite elements.

To show the advantages of the DG Method, an initial classical bang-bang test case is presented. The example demonstrates how to obtain: i) an optimal control solution with h-refinement; and ii) a sub-optimal solution obtained with a uniform time discretization where the switching point lies inside a time element. The second test case is the latching (bang-bang) control of a spar-buoy oscillating water column (OWC) wave energy converter (Henriques et al., 2016d).

The main contributions of the paper are: i) a new numerical solution of OCPs using the Pontryagin's Maximum Principle within the framework of the Discontinuous Galerkin finite element method; ii) approximation of the

control variables with the same basis functions of the state and co-state variables; and iii) a h-refinement algorithm for problems were the switching instant is not know *a priori*.

The paper is organized as follows. A discussion about the need for a continuous solution in time is presented in Section 2 . Section 3 describes the numerical solution of OCPs within the framework of the Pontryagin's Maximum Principle based on the Discontinuous Galerkin Finite Element Method. Section 4 contains results for two bang-bang test cases. Conclusions are drawn in section 5.

2. THE NEED FOR A CONTINUOUS TIME SOLUTION

An OWC is a type of wave energy converter where a hollow structure is open in the bottom to the action of the waves and in the top to the atmosphere through a duct where a turbine is installed, as illustrated in Fig. 1. The wave action compresses and decompresses the air entrapped in the air chamber, resulting in a flow that drives a turbine/generator set. Controlling a latching valve installed in series with the turbine can significantly increase the turbine power output. The control of the valve is of the bang-bang type and is usually called "latching control".

Turbine aerodynamics and mechanical constraints require that the latching valve control can only have two states, $u \in \{0, 1\}$. Due to the physical dimensions and operating mode of the high-speed stop valve, the opening/closing action takes at least $\Delta t = 0.1\,\mathrm{s}$ to execute. For practical purposes, we may assume that the control action occurs instantaneously but it can only happen at the beginning of each time-step. If the time integration is performed considering a time interval of Δt, this constraint is straightforward to handle. However, this approach transforms the original optimal control into a sub-optimal control problem.

In previous works (Henriques et al., 2016a,c), the authors found that significant performance improvements can be achieved with a latching control strategy within a receding horizon framework. However, an undesired effect was found occasionally: the high-speed stop valve is opened/closed intermittently during short periods of time (less than 2 s). This behaviour is not acceptable in practice.

A possible cause for this undesired behaviour was the point-wise computation of the control action as a result of using a discrete time integration method. To fully understand this argument, let us consider the linear second-order initial value problem

$$\dot{\mathbf{x}} = \mathbf{f}(t, \mathbf{x}, \mathbf{u}), \tag{1}$$

subject to the initial conditions

$$\mathbf{x}(0) = \mathbf{x}_0. \tag{2}$$

where $t \in [t_0, t_f]$, $\mathbf{x} = (x_1, \ldots, x_n) \in \mathbb{R}^n$, $\mathbf{f} = (f_1, \ldots, f_n) \in \mathbb{R}^n$ and $\mathbf{u} = \mathbf{u}(t) \in \mathcal{U}$ is the control function. The set $\mathcal{U}$ describes the constraints applied to $\mathbf{u}$.

The goal of the optimal control is to determine $\mathbf{u}$, defined in $[t_0, t_f]$ which maximizes the cost functional J defined as

$$J(\mathbf{u}) = \mathcal{C}_f + \int_{t_0}^{t_f} \mathcal{L}(\mathbf{x}, \mathbf{u})\, \mathrm{d}t, \tag{3}$$

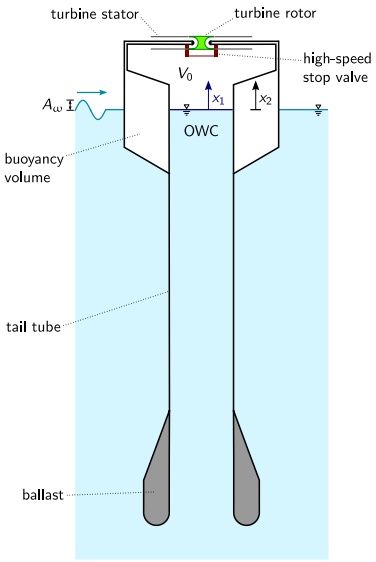

Figure 1. Cut-view of an OWC spar-buoy geometry (not to scale). In the present work, the device is equipped with a linear air turbine and a HSSV in series with the turbine. The HSSV is shown in the closed position.

where $\mathbf{x}_f = \mathbf{x}(t_f)$ and $\mathcal{C}_f = \mathcal{C}(\mathbf{x}_f)$ is the cost associated with the terminal state $\mathbf{x}_f$.

Applying the Pontryagin's Maximum Principle (PMP) along the optimal path $(\mathbf{x}, \mathbf{u}, \boldsymbol{\lambda})$ that maximizes J, leads to the following adjoint equation

$$\dot{\boldsymbol{\lambda}} = \mathbf{g}(t, \mathbf{x}, \mathbf{u}, \boldsymbol{\lambda}) \tag{4}$$

where

$$\mathbf{g}(t, \mathbf{x}, \mathbf{u}, \boldsymbol{\lambda}) = -\nabla_{\mathbf{x}} \mathbf{f}(t, \mathbf{x}, \mathbf{u})^{\mathsf{T}} \boldsymbol{\lambda} - \nabla_{\mathbf{x}} \mathcal{L}(\mathbf{x}, \mathbf{u}), \tag{5}$$

subjected to the terminal condition

$$\boldsymbol{\lambda}_f = \nabla \mathcal{C}_f^{\mathsf{T}}, \tag{6}$$

where $\boldsymbol{\lambda}$ is designated by co-state.

For each t, the Hamiltonian $\mathcal{H}$ defined by

$$\mathcal{H}(t, \mathbf{x}, \mathbf{u}, \boldsymbol{\lambda}) = \boldsymbol{\lambda}^{\mathsf{T}} \mathbf{f}(t, \mathbf{x}, \mathbf{u}) + \mathcal{L}(\mathbf{x}, \mathbf{u}) \tag{7}$$

is maximum for the optimal input $\mathbf{u}$.

In the case where $\mathbf{f}(t, \mathbf{x}, \mathbf{u})$ is a linear or a monotonic function of $\mathbf{u}$ the control is of bang-bang type, see Luenberger (1979). In this case we compute $\mathbf{u}$ that maximizes the Hamiltonian $\mathcal{H}$

$$\max_{\mathbf{u} \in \mathcal{U}} \mathcal{H}(\mathbf{x}, \mathbf{u}, \boldsymbol{\lambda}). \tag{8}$$

Let us split the computational time domain $\Omega = [t_0, t_f]$ in N equally spaced time intervals, $I_e = [t_e, t_{e+1}]$, with $t_{e+1} = t_e + \Delta t$ and $\Delta t = (t_f - t_0)/N$.

For the optimal control strategy we want to determine $\mathbf{u}_n = \mathbf{u}(t_n)$ for $t_0 \leq t_n \leq t_f$ such that $J(\mathbf{u})$ is maximum subjected to the constraint $0 \leq \mathbf{u}_n \leq 1$.

A typical discrete solution of the optimal control problem may be obtained using a 4th-order Runge-Kutta time integration method, following the algorithm depicted in Fig. 2 a). We start by forward time integration of Eq. (1) followed by a backward time integration of Eq. (4). Afterwards, we compute the optimal that maximizes the Hamiltonian (7). The process is repeated until convergence.

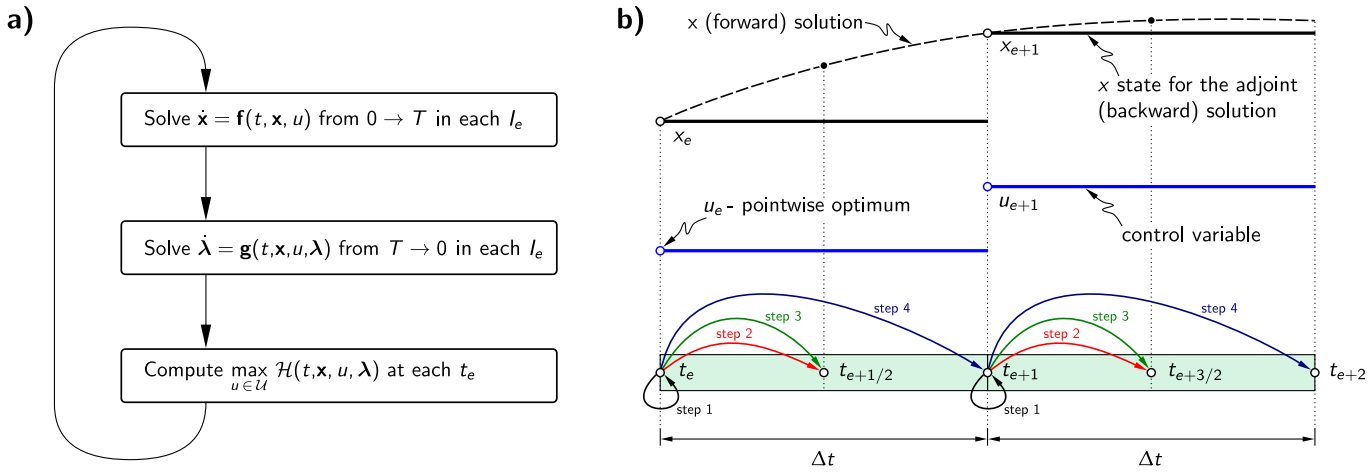

Figure 2. a) Typical sequence solution of the OCP within the framework of the PMP. b) The 4th-order discrete Runge-Kutta time stepping method.

The discrete Runge-Kutta is one of the most popular methods for time integration of Eqs. (1) and (4). The 4th-order Runge-Kutta method is a four step scheme given by

$$\begin{aligned} \mathbf{h}_1 &= \mathbf{f}(t_e,\, \mathbf{x}_e, \mathbf{u}_e)\,, \\ \mathbf{h}_2 &= \mathbf{f}\big(t_e + \tfrac{1}{2}\Delta t,\, \mathbf{x}_e + \tfrac{1}{2}\Delta t\, \mathbf{h}_1, \mathbf{u}_e\big)\,, \\ \mathbf{h}_3 &= \mathbf{f}\big(t_e + \tfrac{1}{2}\Delta t,\, \mathbf{x}_e + \tfrac{1}{2}\Delta t\, \mathbf{h}_2, \mathbf{u}_e\big)\,, \\ \mathbf{h}_4 &= \mathbf{f}(t_e + \Delta t,\, \mathbf{x}_e + \Delta t\, \mathbf{h}_3, \mathbf{u}_e)\,, \end{aligned} \tag{9}$$

$$\mathbf{x}_{e+1} = \mathbf{x}_e + \frac{\Delta t}{6}\left(\mathbf{h}_1 + 2\,\mathbf{h}_2 + 2\,\mathbf{h}_3 + \mathbf{h}_4\right). \tag{10}$$

The result of the Runge-Kutta time integration is a sequence of discrete values $\mathbf{x}$ and $\boldsymbol{\lambda}$ at time instants t_e as shown in Fig. 2 b). Due to the discrete nature of the algorithm, it suffers from three main drawbacks:

- The backward integration of the adjoint equation is performed assuming that $\mathbf{x}$ is piecewise constant in $[t_e, t_{e+1}]$ and equal to $\mathbf{x}_e$.
- The control for the time interval $[t_e, t_{e+1}]$ is computed as function of the point-wise values at t_e, $\mathbf{u}_e(t_e, \mathbf{x}_e, \boldsymbol{\lambda}_e)$.
- If the time interval Δt is not infinitesimal, the optimal control approximation $\mathbf{u}_e$ may not be the optimal in I_e.

To overcome these issues we need a continuous piecewise solution for $\mathbf{x}$ and $\boldsymbol{\lambda}$.

Moreover, the sub-optimal solution $\mathbf{u}$ that maximizes the Hamiltonian $\mathcal{H}$ should be computed as

$$\max_{\mathbf{u} \in \mathcal{U}} \int_{t_e}^{t_{e+1}} \mathcal{H}(t, \mathbf{x}, \mathbf{u}, \boldsymbol{\lambda})\, \mathrm{d}t, \tag{11}$$

instead of the point-wise value

$$\max_{\mathbf{u} \in \mathcal{U}} \mathcal{H}(t_e, \mathbf{x}_e, \mathbf{u}, \boldsymbol{\lambda}_e). \tag{12}$$

3. THE DISCONTINUOUS GALERKIN METHOD

3.1 Weak formulation for the state equations

The Discontinuous Galerkin finite element space is defined as

$$V_h^k \equiv \{v \in L^2(0,T) : v\,|_{I_e} \in P^k(I_e), e = 0, \ldots, N\}, \tag{13}$$

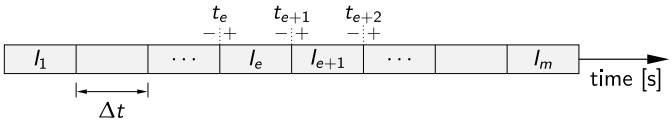

Figure 3. Discretization of the time domain in elements.

where $P^k(I_e)$ is the space of the polynomials in I_e of degree at most k. Although not required, the same degree k of polynomial approximation was used for all the finite elements, I_e, that discretize the domain Ω.

The DG method seeks an approximate solution $x_h \in V_h^k$ of x satisfying (1), such that for any $v_h \in V_h^k$, and all I_e (Huynh, 2011; Shu, 2014),

$$\int_{I_e} v_h \frac{\mathrm{d}x_h}{\mathrm{d}t}\,\mathrm{d}t + v_h(t_e)\,\left[x_h(t_e^+) - x(t_e^-)\right] = \int_{I_e} v_h\, f\,\mathrm{d}t, \tag{14}$$

where the superscripts $+$ and $-$ denote the right and left element boundaries, see Fig. 3.

The jump term defined by

$$x_h(t_e^+) - x(t_e^-) = [\![x]\!]_e\,, \tag{15}$$

serves the purpose of weakly enforcing the left boundary condition $x(t_e^-)$ on element I_e.

3.2 Legendre polynomials

Consider a polynomial approximation of k-th order for x in the element I_e such that

$$\hat{x}_h(\tau) = \sum_{j=0}^{k} p_j(\tau)\,\tilde{x}_{e,j}. \tag{16}$$

Choosing Legendre polynomials, p_j may be obtained using the Rodrigues' formula (Arfken et al., 2013)

$$p_j(\tau) = \frac{1}{j!\,2^j}\left(\frac{\mathrm{d}}{\mathrm{d}x}\right)^j \left(x^2 - 1\right)^j. \tag{17}$$

It can be shown that $p_j(1) = 1$ and $p_j(-1) = (-1)^j$.

3.3 Domain transformation for each finite-element

Introducing in (14) an affine transformation from $t \in I_e$ to $\tau \in [-1, 1]$, we obtain

$$\int_{-1}^{1} \hat{v}_h \frac{\mathrm{d}\hat{x}_h}{\mathrm{d}\tau}\,\mathrm{d}\tau + \hat{v}_h(-1)\,\hat{x}_h(-1^+) - \hat{v}_h(-1)\,\hat{x}(-1^-) = \frac{\Delta t}{2}\int_{-1}^{1} \hat{v}_h\,\hat{f}\,\mathrm{d}\tau, \tag{18}$$

where the hat denotes a function mapped onto a local computational domain, τ, using

$$\tau = \frac{2}{\Delta t_e}(t - t_e) - 1. \tag{19}$$

3.4 System of equations

Equation (18) is applied to all elements I_e of the computational domain Ω. Replacing (16) in (18) and using the set of Legendre polynomials, p_i, as test functions, $\hat{v}_h$, we get a system of algebraic equations

$$\left(A_{ij} + P_{ij}^{-}\right)\tilde{x}_{e,j} = p_i(-1)\,x_{e,j}^{\mathrm{BC}} + b_i, \tag{20}$$

where

$$A_{ij} = \int_{-1}^{1} p_i\,\dot{p}_j\,\mathrm{d}\tau \tag{21}$$

and

$$b_i = \frac{\Delta t}{2}\int_{-1}^{1} p_i\,\hat{f}\,\mathrm{d}\tau. \tag{22}$$

The matrix associated with the inter-element boundary condition are given by

$$P_{ij}^{-} = p_i(-1)\,p_j(-1). \tag{23}$$

The boundary conditions $x_{e,j}^{\mathrm{BC}}$ for each element I_e are given by

$$x_{e,j}^{\mathrm{BC}} = \begin{cases} x_{0,j}, & e = 0, \\ \sum_{j=0}^{k} p_j(+1)\,\tilde{x}_{e-1,j}, & 0 < e \leq N. \end{cases} \tag{24}$$

The integrals appearing in (21) and (22) are computed using the Gauss-Legendre integration rule (Abramowitz and Stegun, 1964) with q points.

The initial value problem (20) is solved starting from the element I_0, integrating sequentially and element-by-element forward in time. Each component of the state vector $\mathbf{x}$ of (1) is computed sequentially.

3.5 Weak form of the adjoint equations

The adjoint equations are integrated backward. The weak formulation for the adjoint equations is similar to (14)

$$\int_{-1}^{1} \hat{v}_h \frac{\mathrm{d}\hat{\lambda}_h}{\mathrm{d}\tau}\,\mathrm{d}\tau + \hat{v}_h(1)\,\left[\lambda(1^+) - \hat{\lambda}_h(1^-)\right] = \frac{\Delta t}{2}\int_{-1}^{1} \hat{v}_h\,\hat{g}\,\mathrm{d}\tau, \tag{25}$$

where the jump term is defined at the right-hand side of the element I_e and defined by

$$\lambda(t_{e+1}^{+}) - \lambda_h(t_{e+1}^{-}) = [\![\lambda]\!]_{e+1}\,. \tag{26}$$

Considering a polynomial approximation of k-th order for λ we get

$$\hat{\lambda}_h(\tau) = \sum_{j=0}^{k} p_j(\tau)\,\tilde{\lambda}_{e,j}. \tag{27}$$

The resulting system of equations is given by

$$\left(A_{ij} - P_{ij}^{+}\right)\tilde{\lambda}_{e,j} = -p_i(+1)\,\lambda_{e,j}^{\mathrm{BC}} + c_i. \tag{28}$$

where

$$c_i = \frac{\Delta t}{2}\int_{-1}^{1} p_i\,\hat{g}\,\mathrm{d}\tau \tag{29}$$

The boundary conditions $\lambda_{e,j}^{\mathrm{BC}}$ for each element I_e are given by

$$\lambda_{e,j}^{\mathrm{BC}} = \begin{cases} \lambda_{T,j}, & e = N \\ \sum_{j=0}^{k} p_j(-1)\,\tilde{\lambda}_{e+1,j}, & 0 \leq e < N \end{cases}. \tag{30}$$

3.6 Maximization of the Hamiltonian function

Following the typical approach of the finite element methods, we approximate each component of the vector of control variables $\mathbf{u}$ with a Legendre polynomial such that

$$\hat{u}_h(\tau) = \sum_{j=0}^{k} p_j(\tau)\,\tilde{u}_{e,j}. \tag{31}$$

The optimal solution $\mathbf{u}(t)$ is computed by maximizing the integral of the Hamiltonian, $\mathcal{H}$, in each time interval, I_e, using (11).

In the case of continuous control, a standard gradient based optimization algorithm can be used to compute the $\tilde{u}_{e,j}$ that maximizes (32) in each I_e. The derivative of (11) in order to $\tilde{u}_{e,j}$, usually required by the optimization algorithms, is given, for each element, by

$$\frac{\Delta t_e}{2}\int_{-1}^{1} \frac{\partial \mathcal{H}}{\partial \hat{u}_h}\frac{\partial \hat{u}_h}{\partial \tilde{u}_{e,j}}\,\mathrm{d}\tau, \tag{32}$$

where

$$\frac{\partial \hat{u}_h}{\partial \tilde{u}_{e,j}} = p_j(\tau). \tag{33}$$

For the present bang-bang optimal control problems, we assume a constant value of $\hat{u}_h$ in each element, I_e. In our finite element context, a constant value of $\hat{u}_h$ in each element, I_e, is equivalent to a zero degree polynomial approximation

$$\hat{u}_h(\tau) = p_0(\tau)\,\tilde{u}_{e,0}. \tag{34}$$

4. RESULTS

Before considering the main problem, related to an OWC, a case study is presented in order to illustrate, in a simpler setting, the main ideas of the method.

4.1 Case test 1: A bang-bang OCP with analytical solution

The population of wasps in a colony is formed by two cases: workers, x, and reproductives, p. From an evolutionary perspective, in each year, the goal of the colony is to maximize the number of reproductive elements. The problem of maximizing the number of reproductives can be modelled by the following equation (Luenberger, 1979)

$$\dot{x} = bux - \mu x, \tag{35}$$

Algorithm 1 h-Refinement for bang-bang optimal control problems

1: **for** $e \in \{0, \ldots, N-1\}$ **do**
2: **if** ($e > 0$ **and** $u_{e-1} != u_e$) **or** ($e < N-1$ **and** $u_e != u_{e+1}$) **then**
3: Split element I_e at the zeros of $(\partial\mathcal{H}/\partial u)$
4: **end if**
5: **end for**

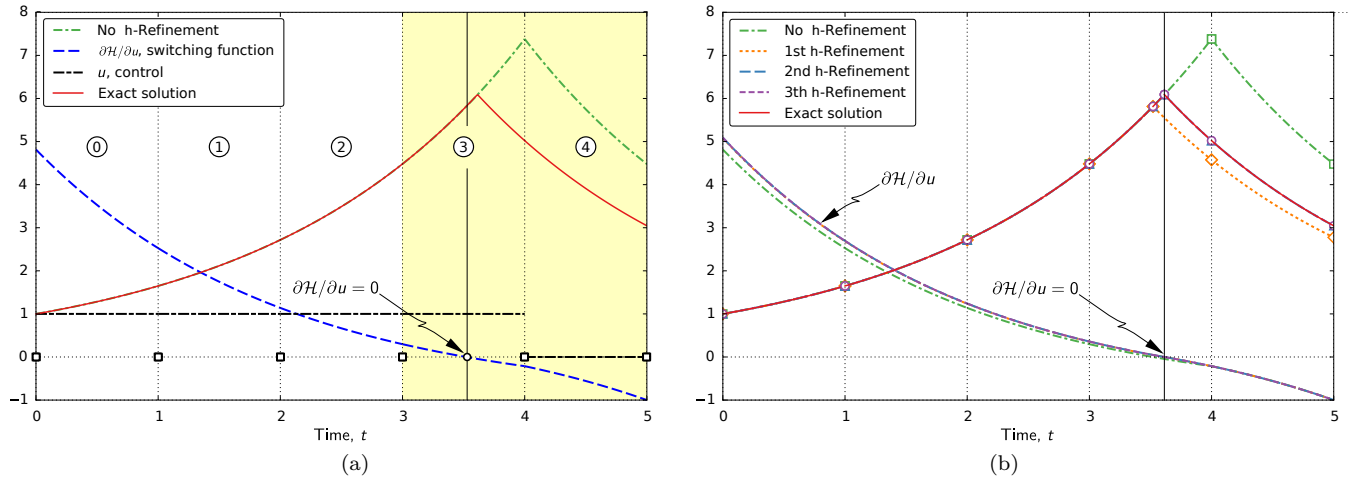

Figure 4. h-refinement algorithm for a third-order Legendre polynomial. a) Initial solution without h-refinement considering 5 elements of time length 1 s, $0 \leq j \leq 4$. b) Comparison between the analytical solution and the 3 levels required to converge the h-refinement algorithm.

where b, c and μ are positive constants. The optimal control problem is to maximize

$$\mathcal{L}(x,u) = c\,(1-u)\,x, \tag{36}$$

in the fixed time interval $t \in [0,T]$, subject to the constraint $u \in [0,1]$ and the initial condition is $x(0) = 1$.

The adjoint equation is given by

$$\dot{\lambda} = -\,(bu-\mu)\,\lambda - c\,(1-u)\,, \tag{37}$$

with $\lambda(T) = 0$. The Hamiltonian is

$$\mathcal{H} = ((\lambda b - c)\,u + (c - \lambda\mu))\,x. \tag{38}$$

It can be shown that for $t = T$ we have $u(T) = 0$, see Luenberger (1979). Since the Hamiltonian is linear in u, the optimal control solution is of the bang-bang type.

For the present solution we will assume that the control u is constant for each time step Δt. The switching function is, for each time interval I_e,

$$u(I_e) = \begin{cases} 1, & \displaystyle\int_{t_e}^{t_{e+1}} \frac{\partial\mathcal{H}}{\partial u}\,\mathrm{d}t > 0, \\ 0, & \text{otherwise.} \end{cases} \tag{39}$$

The results for the optimal control computed with $b = 1$, $c = 1$ and $\mu = \frac{1}{2}$ are plotted in Fig. 4 for several $\Delta t = T/N$. For the case considered $b = 1$, $c = 1$, $\mu = 0.5$ and $T = 5$ s. The analytical solution can be found in Luenberger (1979).

Fig. 4 a) shows that forcing the time element boundary to be at the switching instant a has a major effect on the numerical results. By applying the h-refinement algorithm 1, the switching instant can be computed with a prescribed degree of accuracy, see Fig. 4 b). Algorithm 1 basically splits the elements at the zero crossing points of $(\partial\mathcal{H}/\partial u)$.

4.2 Case test 2: Latching (bang-bang) control of a Spar-buoy OWC

The spar-buoy (floater and tail tube) was named here as body 1, see Fig. 1. The air-water interface is modelled as an imaginary weightless rigid piston denoted as body 2. A complete description of the non-linear numerical model can be found in Henriques et al. (2016b,d,e). The spar-buoy OWC oscillates essentially in heave. Let x_i be the coordinates of body i for the heave motion, with $x_i = 0$ at the equilibrium position and the x_i-axes pointing upwards. A simplified first-order ordinary system of equations that describes the system is given by

$$\dot{\mathbf{x}} = \mathbf{f}(t, \mathbf{x}), \tag{40}$$

where

$$\mathbf{x} = (\,v_1 \;\; v_2 \;\; x_1 \;\; x_2 \;\; p^*\,)^{\mathsf{T}}. \tag{41}$$

$$\mathbf{f}(t,\mathbf{x}) = (f_1 \;\; f_2 \;\; v_1 \;\; v_2 \;\; f_p)^{\mathsf{T}}, \tag{42}$$

and $v_1 = \dot{x}_1$, $v_2 = \dot{x}_2$. The functions f_1 and f_2 are linear functions of $\mathbf{x}$ given by

$$f_1 = M_2^*\mathcal{F}_1 - A_{12}^*\mathcal{F}_2, \tag{43}$$
$$f_2 = M_1^*\mathcal{F}_2 - A_{21}^*\mathcal{F}_1, \tag{44}$$

with

$$\mathcal{F}_1 = -K_1\,x_1 + K_p\,p^* + F_{d1} - R_{11}, \tag{45}$$
$$\mathcal{F}_2 = -K_2\,x_2 - K_p\,p^* + F_{d2}. \tag{46}$$

Here $M_i = m_i + A_{ii}^{\infty}$, $\mathcal{D} = (M_1M_2 - A_{12}^{\infty}A_{21}^{\infty})^{-1}$, $M_i^* = \mathcal{D}M_i$, $A_{ij}^* = \mathcal{D}A_{ij}^{\infty}\,m_i$, is the mass of body i, A_{ij}^{∞} represents the limiting value at infinite frequency of the added mass of body i as affected by the motion of body j, $F_{\mathrm{d},i}$ is the hydrodynamic excitation force on body i, see Henriques et al. (2016e) for further details. The stiffness constants are defined by $K_1 = \varrho_{\mathrm{w}}gS_1$, $K_2 = \varrho_{\mathrm{w}}gS_2$ and $K_p = S_2\,p_{\mathrm{at}}$, where g is the acceleration of gravity, ϱ_{w} is water density,

Algorithm 2 Iterative method to solve the state-adjoint-control set of equations

Initialize $\mathbf{x}_e^0$, $\boldsymbol{\lambda}_e^0$ and u_e^0, $\forall e \in \{0,\dots,N\}$
$n \leftarrow 0$
repeat ▷ outer loop
  $n \leftarrow n+1$
  for $e \in \{0,\dots,N\}$ **do** ▷ loop initialization
    $\mathbf{x}_e^{n,0} \leftarrow \mathbf{x}_e^{n-1}$
    $\boldsymbol{\lambda}_e^{n,0} \leftarrow \boldsymbol{\lambda}_e^{n-1}$
    $u_e^{n,0} \leftarrow u_e^{n-1}$
  end for
  $m \leftarrow 0$
  repeat ▷ inner loop to solve for $\mathbf{x}$
    $m \leftarrow m+1$
    for $e \in \{0,\dots,N\}$ **do** ▷ forward iteration
      Solve $\dot{\mathbf{x}}_e^{n,m} = \mathbf{f}\left(t, \mathbf{x}_e^{n,m-1}, u_e^{n-1}\right)$
    end for
  until $\left\|\mathbf{x}_e^{n,m} - \mathbf{x}_e^{n,m-1}\right\|_\infty < \epsilon_x,\ \forall e \in \{0,\dots,N\}$
  $\mathbf{x}_e^n \leftarrow \mathbf{x}_e^{n-1} + \alpha\left(\mathbf{x}_e^{n,m} - \mathbf{x}_e^{n-1}\right)$ ▷ under-relaxation
  $m \leftarrow 0$
  repeat ▷ inner loop to solve for $\boldsymbol{\lambda}$ and u
    $m \leftarrow m+1$
    for $e \in \{N,\dots,0\}$ **do** ▷ backward iteration
      Solve $\dot{\boldsymbol{\lambda}}_e^{n,m} = \mathbf{g}\left(t, \mathbf{x}_e^n, \boldsymbol{\lambda}_e^{n,m-1}, u_e^{n,m-1}\right)$
      $s \leftarrow \int_{I_e} S(\mathbf{x}_e^n, \boldsymbol{\lambda}_e^{n,m}, u_e^{n,m-1})\,\mathrm{d}t$
      if $s > 0$ **then** ▷ test switching function
        $u_e^{n,m} \leftarrow 1$
      else
        $u_e^{n,m} \leftarrow 0$
      end if
    end for
  until $\left\|\boldsymbol{\lambda}_e^{n,m} - \boldsymbol{\lambda}_e^{n,m-1}\right\|_\infty < \epsilon_\lambda,\ \forall e \in \{0,\dots,N\}$
  $\boldsymbol{\lambda}_e^n \leftarrow \boldsymbol{\lambda}_e^{n-1} + \alpha\left(\boldsymbol{\lambda}_e^{n,m} - \boldsymbol{\lambda}_e^{n-1}\right)$ ▷ under-relaxation
  $u_e^n \leftarrow u_e^{n,m}$
until $\left\|\mathbf{x}_e^n - \mathbf{x}_e^{n-1}\right\|_\infty < \epsilon_x,\ \forall e \in \{0,\dots,N\}$

S_i is the annular cross sectional area of body i and p_{at} is the atmospheric pressure. In the present work, we only consider the radiation of body 1, R_{11}, computed using a constant hydrodynamic coefficient model (Kurniawan et al., 2011)

$$R_{11} = B_{11}(\omega_p)\, v_1, \tag{47}$$

where $B(\omega)$ is the radiation damping in the frequency domain and ω_p is the wave spectral peak frequency.

In the present work, only irregular waves were considered. Under regular (monochromatic) waves, latching control is simply a mere repetition of the optimal control action for a single period. Assuming linear water wave theory, the hydrodynamic excitation force is obtained as a superposition of N angular frequency components, ω_m,

$$F_{\mathrm{d},i} = \sum_{m=1}^{N} \Gamma_i(\omega_m)\, A_m \cos(\omega_m t + \phi_{i,m} + \phi_r), \tag{48}$$

where $\Gamma(\omega_m)$ is the excitation force coefficient, A_m is the frequency-dependent wave amplitude, $\phi_{i,m}$ is the phase response of body i at the angular frequency ω_m and ϕ_r is a random phase. The frequencies ω_m result from a discretized Pierson-Moskowitz spectrum, see Goda (2000); Henriques et al. (2012) for details. Typically, ocean waves have typical periods, T_w, between 6 s and 16 s. As the considered time intervals, Δt, are much smaller that the typical wave periods, $\Delta t \ll T_w$, the h-refinement algorithm was not used for this test case. The optimal control was computed considering a time interval of $T = 1200$ s.

The dimensionless relative pressure oscillation inside the air chamber is defined as

$$p^* = \frac{p}{p_{\mathrm{at}}} - 1, \tag{49}$$

where p is the instantaneous pressure inside the air chamber. The last entry of (42) is a non-linear function of $\mathbf{x}$ defined by

$$f_p = -\gamma\,(p^*+1)\,\frac{\dot{V}_{\mathrm{c}}}{V_{\mathrm{c}}} - \gamma\,(p^*+1)^{\beta}\,\frac{Q_{\mathrm{turb}}}{V_{\mathrm{c}}}\,u. \tag{50}$$

Here $V_{\mathrm{c}} = V_0 + S_2\,(x_1 - x_2)$ is the instantaneous volume of air inside the chamber, V_0 is the volume at hydrostatic conditions, and S_2 is the area of the OWC free surface. The constant $\gamma = 1.4$ is the specific heat ratio for the air and $\beta = 1 - 1/\gamma$. The volumetric flow rate through the turbine, Q_{turb}, is a function of the pressure difference between the air chamber and the atmosphere and the turbine rotational speed. The control u models a latching valve actuated in series with the turbine. Since (42) is a linear function of u, the optimal control is of the bang-bang type.

The performance characteristics of the turbine are usually presented in dimensionless form. Here we consider a lossless turbine where the dimensionless pressure head, Ψ and dimensionless flow rate, Φ, are related by (see Dick (2015); Dixon and Hall (2013))

$$\Phi = \mathrm{sign}(\Psi)\, K_t |\Psi|^n, \tag{51}$$

where

$$\Psi = \frac{p_{\mathrm{at}}\, p^*}{\varrho_{\mathrm{at}}\, \Omega^2\, d^2}, \tag{52}$$

$$\Phi = \frac{Q_{\mathrm{turb}}}{\Omega\, d^3}. \tag{53}$$

In Eqs. (52) and (53), Ω is the turbine rotational speed (in radians per unit time) and d is the turbine rotor diameter. Assuming a large turbine inertia, a constant rotational speed, Ω, model was adopted. The atmospheric air density is denoted as ϱ_{at}. Furthermore, we will assume that the turbine operates at a constant rotational speed and $n = 3/5$ is a turbine type dependent constant.

The optimal control aims to maximize the time-averaged turbine power output,

$$J(u) = \int_0^T \left(\frac{u\,\Psi\Phi}{T} + \varepsilon\,(1-u)^2\right)\mathrm{d}t, \tag{54}$$

where $(1-u)^2$ is a regularization term and ε is a small positive constant. The regularization term is as a threshold value to avoid opening the latching valve when the available pneumatic power, $\Psi\Phi$, is too small. The switching function is given by

$$\frac{\partial \mathcal{H}}{\partial u} = -\lambda_5 \gamma (p^*+1)^{\beta} \frac{Q_{\mathrm{turb}}}{V_{\mathrm{c}}} + \frac{\Psi\Phi}{T} \;+\; 2\varepsilon(u-1), \tag{55}$$

where λ_5 is the fifth entry of $\boldsymbol{\lambda}$. The control is computed using (39). In the present case, Eq. (39) has no singular arcs as the integral is always different from zero. The integrand is only zero at the points where the pressure crosses zero, $p^* = 0 \Rightarrow \Psi = \Phi = Q_{\mathrm{turb}} = 0$. Due to the

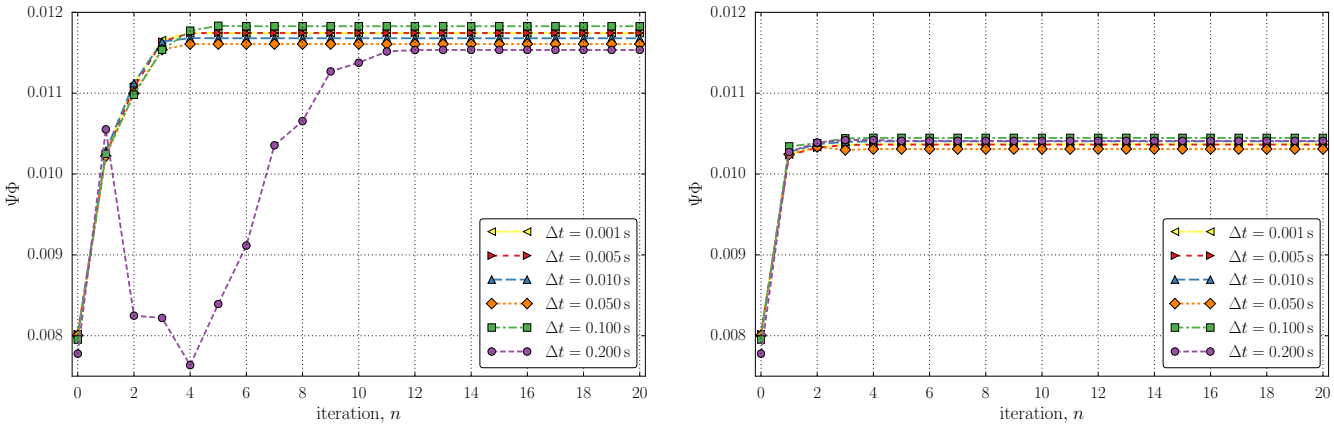

(a) (b)

Figure 5. Dimensionless time-averaged turbine power, $\Psi\Phi$ as function of the time iteration for several time steps, Δt. Results for (a) $\varepsilon = 0.0001$ and (b) $\varepsilon = 0.05$. The value of $\Psi\Phi$ for iteration $n = 0$ corresponds to the uncontrolled case.

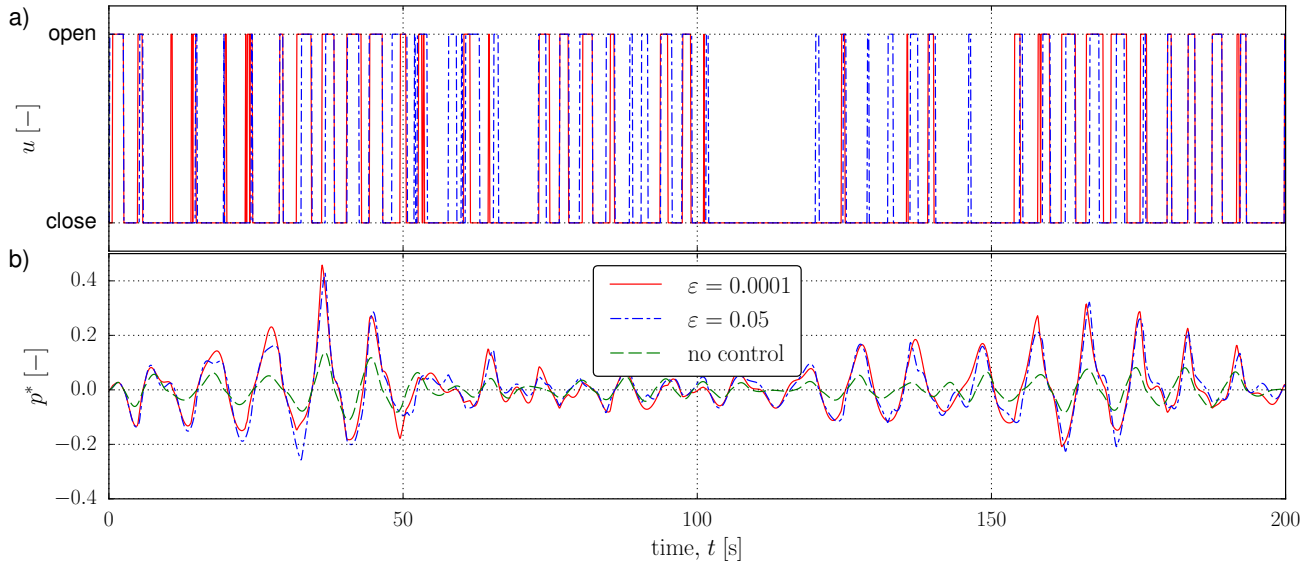

Figure 6. Comparison of (a) the control, u, and (b) the dimensionless relative pressure, p^*, as function of the time, for $\varepsilon = 0.0001$ and $\varepsilon = 0.05$. For comparison, the results for p^* without latching control ($u = 1$) are also plotted. In all cases, a time step of $\Delta t = 0.1\,\mathrm{s}$ was selected and only the first 200 s are plotted.

oscillatory nature of the excitation force - the ocean waves - this event only happens typically twice in each wave cycle.

The overall solution method for the present OCP is described in Algorithm 2. The state, co-state and control variables are solved using a segregated solution method with under-relaxation to improve convergence. The dimensionless time-averaged turbine power output is plotted in Figure 5. A sea-state with an energy period of $T_\mathrm{e} = 8\,\mathrm{s}$ and a significant wave height of $H_\mathrm{s} = 2\,\mathrm{m}$ was assumed. Figures 5 a) and b) shows the importance of the choice of ε for the turbine power output and the convergence rate of the optimal control. A smaller value of ε increases the time-averaged turbine power output but also increases the number of iterations required to achieve convergence. This effect is clear in Fig. 5 a) for the case where $\Delta t = 0.2\,\mathrm{s}$. The increase of ε also reduces variance of the power output as functions of the time step. For $\varepsilon = 0.0001$, the relative turbine power output gains are about 46%, while in the case of $\varepsilon = 0.05$ the gains are only 30%.

The time series results of the control and the dimensionless relative pressure are plotted in Fig. 6. For comparison, the pressure is also plotted for the case without latching control. Figure 6 a) shows that for the smallest ε the latching valve operates in several occasions intermittently for short time intervals. The regularization effect of increasing ε may be used to achieve a more reliable operation of the turbine although reducing the time-averaged turbine power output. From Fig. 6 b) we check that the latching control increases the power output by increasing significantly the pressure peaks. In the case of the lower ε this behaviour is enhanced. Interestingly, when the valve is closed for longer time-periods, pressure peaks have a larger increase than the uncontrolled case.

5. CONCLUSIONS

The current paper demonstrates the capabilities of the Discontinuous Galerkin method to solve optimal and sub-optimal control problems within the framework of the Pontryagin's Maximum Principle. Adaptive mesh h-refinement was exploited to obtain high-accurate bang-bang solutions without prior knowledge of the switching instant. Latching control of a spar-buoy OWC demonstrated the capabilities of the DG in the numerical solution of a bang-bang sub-optimal control where: i) time-step is fixed and non-infinitesimal; ii) the control command is only applied at the beginning of each time-step; and iii) the number of switching instants is very large and not known *a priori*. Due to the high-oscillatory system dynamics of the spar-buoy OWC, it was necessary to include a regularization term to improve the convergence rate. The results show that the DG method can be seen as an efficient alternative to the well-known Pseudo-Spectral methods.

ACKNOWLEDGEMENTS

I thank my supervisors Professors António Falcão and João Henriques for all their patience and support provided during the execution of this work. My aunt Teresa Vilhena for having read the thesis and patiently helped me to correct the many orthographic errors in the first version. I would like to thank my colleagues for their interest in the theme addressed by this work and the moral support. My family for all the unconditional support and patience ever present throughout my life.

REFERENCES

Abramowitz, M. and Stegun, I.A. (1964). *Handbook of Mathematical Functions with Formulas, Graphs, and Mathematical Tables*. Dover, New York, 9th printing edition.

Arfken, G.B., Weber, H.J., and Harris, F.E. (2013). *Mathematical Methods for Physicists*. Academic Press, Boston, 7th edition. doi:10.1016/B978-0-12-384654-9.00030-X.

Boucher, R., Kang, W., and Gong, Q. (2014a). Discontinuous Galerkin optimal control for constrained nonlinear problems. In *11th IEEE International Conference on Control Automation (ICCA)*, 84–89. doi:10.1109/ICCA.2014.6870900.

Boucher, R., Kang, W., and Gong, Q. (2014b). Feasibility of the galerkin optimal control method. In *53rd IEEE Conference on Decision and Control*, 6671–6676. doi:10.1109/CDC.2014.7040436.

Dick, E. (2015). *Fundamentals of Turbomachines*, volume 109 of *Fluid Mechanics and Its Applications*. Springer Netherlands. doi:10.1007/978-94-017-9627-9.

Dixon, S.L. and Hall, C.A. (2013). *Fluid mechanics and thermodynamics of turbomachinery*. Butterworth-Heinemann, Oxford, 7th edition edition.

Goda, Y. (2000). *Random Seas and Design of Maritime Structures*. World Scientific Publishing, Singapure, 2nd edition.

Henriques, J.C.C., Gato, L.M.C., Falcão, A.F.O., Robles, E., and Faÿ, F.X. (2016a). Latching control of a floating oscillating-water-column wave energy converter. *Renewable Energy*, 90, 229–241. doi:10.1016/j.renene.2015.12.065. URL `http://dx.doi.org/10.1016/j.renene.2015.12.065`.

Henriques, J.C.C., Gato, L.M.C., Falcão, A.F.O., Robles, E., and Faÿ, F.X. (2016b). Latching control of a floating oscillating-water-column wave energy converter. *Renewable Energy*, 90, 229 – 241. doi:10.1016/j.renene.2015.12.065.

Henriques, J.C.C., Gato, L.M.C., Lemos, J.M., Gomes, R.P.F., and Falcão, A.F.O. (2016c). Peak-power control of a grid-integrated oscillating water column wave energy converter. *Energy*, 109, 378–390. doi:10.1016/j.energy.2016.04.098. URL `http://dx.doi.org/10.1016/j.energy.2016.04.098`.

Henriques, J.C.C., Gato, L.M.C., Lemos, J.M., Gomes, R.P.F., and Falcão, A.F.O. (2016d). Peak-power control of a grid-integrated oscillating water column wave energy converter. *Energy*, 109, 378 – 390. doi:10.1016/j.energy.2016.04.098.

Henriques, J.C.C., Gomes, R.P.F., Gato, L.M.C., Falcão, A.F.O., Robles, E., and Ceballos, S. (2016e). Testing and control of a power take-off system for an oscillating-water-column wave energy converter. *Renewable Energy*, 85, 714 – 724. doi:10.1016/j.renene.2015.07.015.

Henriques, J.C.C., Lopes, M.F.P., Gomes, R.P.F., Gato, L.M.C., and Falcão, A.F.O. (2012). On the annual wave energy absorption by two-body heaving WECs with latching control. *Renewable Energy*, 45, 31 – 40. doi:10.1016/j.renene.2012.01.102.

Huynh, H.T. (2011). Collocation and Galerkin time-stepping methods. Technical report, NASA Technical Memoradum /TM-2011-216340. URL `http://ntrs.nasa.gov/search.jsp?R=20110014969`.

Kraft, K. (2008). *Adaptive Finite Element Methods for Optimal Control Problems*. Licentiate thesis, Chalmers University of Technology and Göteborg University. URL `http://www.math.chalmers.se/Math/Research/Preprints/2008/1.pdf`.

Kurniawan, A., Hals, J., and Moan, T. (2011). Assessment of time-domain models of wave energy conversion systems. In *Proc 9th European Wave Tidal Energy Conf, Southampton, U.K.*

Luenberger, D.G. (1979). *Introduction to dynamic systems: theory, models, and applications*. J. Wiley & Sons, New York, Chichester, Brisbane.

Naveh, Y., Bar-Yoseph, P.Z., and Halevi, Y. (1999). Nonlinear modeling and control of a unicycle. *Dynamics and Control*, 9(4), 279–296. doi:10.1023/A:1026481216262.

Shu, C.W. (2014). Discontinuous Galerkin method for time-dependent problems: Survey and recent developments. In X. Feng, O. Karakashian, and Y. Xing (eds.), *Recent Developments in Discontinuous Galerkin Finite Element Methods for Partial Differential Equations: 2012 John H Barrett Memorial Lectures*, 25–62. doi:10.1007/978-3-319-01818-8_2.